

BBN with Late Electron-Sterile Neutrino Oscillations - The Finest Leptometer

D. Kirilova,¹

¹Institute of Astronomy and NAO, BAS, Bulgaria

November 4, 2018

Abstract

A relic lepton asymmetry orders of magnitude bigger than the baryon one may hide in the relic neutrino background. No direct theoretical or experimental limitations on its magnitude and sign are known. Indirect cosmological constraints exist ranging from $|L| < 0.01$ to $L < 10$. We discuss a BBN model with late electron-sterile neutrino oscillations which is a fine leptometer - it is capable of feeling extremely small relic lepton asymmetry - $|L| > 10^{-8}$. This sensitivity is achieved through the influence of such small L on the neutrino oscillations, suppressing or enhancing them, and thus changing the primordially produced ${}^4\text{He}$. The influence of L on nucleons freezing in pre-BBN epoch is numerically analyzed in the full range of the oscillation parameters of the model and for $L \geq 10^{-10}$. The case of oscillations generated asymmetry by late electron-sterile oscillations and its effect on primordial ${}^4\text{He}$ is also briefly discussed.

1 Introduction

Lepton asymmetry of the Universe is usually defined as $L = (N_l - N_{\bar{l}})/N_\gamma$, where N_l is the number density of leptons, and $N_{\bar{l}}$ of antileptons, while N_γ is the number density of photons. In case of equilibrium $\xi = \mu/T$, the degeneracy parameter, is used instead as a qualitative measure of the lepton asymmetry.

It is traditionally assumed that the lepton asymmetry is of the order of the baryon one, which is measured precisely by different independent means (BBN, CMB data) to be $\beta = (N_b - N_{\bar{b}})/N_\gamma \sim 6 \cdot 10^{-10}$. However, actually big L may reside in the neutrino sector ¹ and hence, L may be many orders of magnitude larger than β . Therefore, L is defined mainly by the sum of the asymmetries in the different neutrino sectors $L \sim \sum L_{\nu_i}$. Direct measurements of the lepton asymmetry magnitude and sign have not been done yet. There are available just indirect indications and constraints.

Studying L of the Universe is intriguing and important because of many reasons. Just a short list of some of them reads:

- A significant cosmological effect of L might be expected, having in mind that neutrinos are abundant and large L may be contained in the neutrino sector.

¹Universal charge neutrality implies that the lepton asymmetry in the electron sector is $L_e \sim \beta$.

- Precise determination of neutrino properties is of cosmological importance. As far as the uncertainty of neutrino characteristics leads to large systematic errors in the estimation of cosmological parameters obtained from CMB data. Therefore, knowledge about L and its nature would help to determine them more precisely.
- Studying L and its cosmological influence provides, on the other hand, an opportunity to use cosmology as a probe of neutrino properties.
- There exist different mechanisms of generation of L , and among them is the natural possibility of amplifying the neutrino asymmetry by neutrino active-sterile resonant oscillations in CP -asymmetric plasma of the early Universe [1, 2].
- Planck will soon be able to better constrain L , namely Planck will measure the radiation content at CMB decoupling with a precision $\delta N_{eff} = \pm 0.26$, i.e. it will be able to measure with this precision the eventual L contribution to the radiation content. Besides, in case $\xi > 2$ Planck will be able to detect small neutrino mass of the order of ~ 0.07 eV because L enhances the effect of the mass.
- Today it is reasonable to study L , also as a possible solution of the recently found cosmological preference or/and indication for additional relativistic density [3]. Namely, recent measurements of primordially produced 4He Y_p [4] and CMB measurements of Y_p [5] point to an effective number of the relativistic degrees of freedom at the BBN epoch $N_{BBN} = 3.8^{+0.8}_{-0.7}$, at the CMB formation epoch $N_{CMB} = 4.34^{+0.86}_{-0.88}$ at 68%, and on the basis of LSS survey data $N_{LSS} = 4.8^{+1.9}_{-1.8}$ at 95%, i.e. higher values than previously estimated ones and higher than the theoretically predicted standard value for 3 neutrino species $N_{eff} = 3.046$.
- Moreover, recent analysis of the combined neutrino oscillation data, including LSND and Mini-Boone requires 1 or 2 additional low mass sterile neutrinos ν_s , participating into oscillations with flavor neutrinos with higher mass differences values, than the ones required by solar and atmospheric neutrino oscillations experiments. These light ν_s brought into equilibrium by oscillations with active neutrinos may be a successful explanation of the excess relativistic density. Besides, it is known that such active-sterile oscillations in the resonant case may generate L in the CP -asymmetric plasma of the Universe.
- Knowledge about L magnitude and sign is relevant for cosmological models with leptonic domains, for inhomogeneous BBN models, baryogenesis through leptogenesis issues, etc.
- Determining L at BBN epoch would allow testing the assumption that sphalerons equilibrate lepton and baryon asymmetries.
- Particularly concerning neutrino oscillations: Due to the fact that L is capable of suppressing and inhibiting or enhancing neutrino oscillations, determining L will enlighten our knowledge about their cosmological role.

In the next section lepton asymmetry effects on processes in the Universe and some of the based on them cosmological constraints on L are shortly discussed. In section 3 the interplay between small lepton asymmetry and electron-sterile neutrino oscillations $\nu_e \leftrightarrow \nu_s$, effective after neutrino decoupling, is described in terms of general kinetic equations for oscillating neutrinos and numerically analyzed. In section 4 the results of our numerical analysis of the influence of relic L and oscillations generated L on primordial production of 4He in case of late $\nu_e \leftrightarrow \nu_s$ oscillations are presented.

2 Knowledge about Lepton Asymmetry

Cosmic neutrino Background has not been detected yet, hence L is measured/constrained only indirectly through its effect on other processes, which have left observable traces in the Universe, like the abundances of light elements produced in BBN, Cosmic Microwave Background, LSS, etc. (see for example the reviews [6] – [9]). Recently it was found possible to obtain an information about L from QCD transition, on the basis of L effect at QCD epoch [16]. Below we review the main cosmological effects of L and some of the recent cosmological constraints on L magnitude and sign.

2.1 Lepton Asymmetry Effects

A. Energy density increase.

A well-known cosmological effect of L is the increase of the radiation energy density, which is usually expressed in terms of the increase of the effective number of the relativistic degrees of freedom

$$\rho_r = \rho_\gamma + \rho_\nu = [1 + 7/8(4/11)^{4/3} N_{eff}] \rho_\gamma$$

where ρ_γ and ρ_ν are the photon and neutrino energy densities, correspondingly. In equilibrium L may be expressed as usual through the chemical potential μ or degeneracy parameter $\xi = \mu/T$:

$$L = 1/12\zeta(3) \sum_i T_{\nu_i}^3 / T_\gamma^3 (\xi_{\nu_i}^3 + \pi^2 \xi_{\nu_i})$$

The increase of N_{eff} due to L is

$$\Delta N_{eff} = 15/7 [(\xi/\pi)^4 + 2(\xi/\pi)^2].$$

The increase of the radiation density due to L speeds up the Universe expansion $H = (8/3\pi G\rho)^{1/2}$, delays matter/radiation equality epoch, changes the decoupling temperature of neutrino, which on their turn influence BBN, CMB and the evolution of the density perturbations, i.e. formation of structures in the Universe.

Particularly well studied is L effect on BBN. The increase of the cooling rate of the Universe due to L , leads to earlier freezing of the reactions governing neutron-to-proton ratio n/p , i.e. leads to higher freezing ratio $(n/p)_f$, which reflects in higher D and 4He abundances.

B. Direct kinetic effect.

Besides its dynamical effect, lepton asymmetry with a magnitude $|L| > 0.01$ in the ν_e sector exerts also a direct kinetic effect on the n-p kinetics and on BBN, because the ν_e participates in the reactions interconverting neutrons and protons. In this case the effect on BBN and the outcome of the light elements is L sign dependent.

As is obvious, $L > 0$ in the pre-BBN epoch would result into reduction of $(n/p)_f$ and thus leads to light element underproduction, while $L < 0$ would lead to their overproduction. Degenerate BBN has been thoroughly studied (see for example pioneer papers ref. [13]).

An empirical formula, which provides a fairly good fit (see for example ref. [11]), presents the dependence of the produced primordially 4He , Y_p , on the discussed dynamical and kinetic effect of L :

$$Y_p \sim (0.2482 \pm 0.0006) + 0.0016\eta_{10} + 0.013\Delta N_{eff} - 0.3\xi_{\nu_e}$$

C. Indirect kinetic effect due to asymmetry-oscillations interplay

Small L , $|L| \ll 0.01$, that has negligible A and B effects, in case of late $\nu_e \leftrightarrow \nu_s$ oscillations may considerably influence oscillating ν_e , namely change its evolution, number density, energy distribution, oscillation pattern and thus through ν_e influence BBN kinetics [2, 17]. The effect of small relic L and nonresonant $\nu_e \leftrightarrow \nu_s$ oscillations effective after neutrino decoupling on BBN has been first studied in

ref. [17]. It was found that $L < 10^{-7}$ is destroyed by oscillations, while $L \geq 10^{-7}$ may enhance or suppress oscillations and through them influence primordially produced elements (see also ref. [20]).²

On the other hand active-sterile oscillations may induce neutrino-antineutrino asymmetry growth during the resonant transfer of neutrinos [1, 2, 18, 19]. The case of weak mixing and relatively big mass differences $\delta m^2 > 10^{-4}$ eV² was discussed first in ref. [1], while the case of asymmetry generated at relatively big mixing and small mass differences $\delta m^2 < 10^{-7}$ eV² was first found in ref. [2]. This dynamically produced asymmetry exerts back effect on oscillating neutrino and changes its oscillation pattern.³ There exists another possibility: when L growth is not high enough to have a direct L kinetic effect on the synthesis of light elements, it can effect indirectly BBN through its effect on oscillating neutrinos. In the case of resonant $\nu_e \leftrightarrow \nu_s$ oscillation effective after neutrino decoupling neutrino-antineutrino asymmetry is amplified by not more than 5 orders of magnitude from an initial value of the order of the baryon one [19]. Oscillations generated asymmetry suppresses oscillations at small mixing angles, leading to noticeable decrease of ${}^4\text{He}$ production at these mixing angles. The effect of small L generated by oscillations on ${}^4\text{He}$ abundance and on cosmological constraints on oscillations was analyzed in ref. [2, 19, 20].

In conclusion, very small asymmetries $10^{-7} < L \ll 0.01$, either relic or produced in active-sterile oscillations, may considerably influence oscillating electron neutrino and through it Y_p and BBN. In the next sections we study numerically this special case of influence of small L on oscillating neutrino and on BBN and show that BBN produced ${}^4\text{He}$ feels extremely small L and represents now the finest known "leptometer". For comparison, in the next subsection we present first the available cosmological constraints on L coming from BBN with flavor oscillations present.

2.2 Lepton Asymmetry Constraints

At present BBN provides the most stringent constraints on L . There exist numerous papers on the subject. I list here only the results of more recent work. For more information and reference of earlier papers see the review paper [6].

In case of equilibration of the neutrino oscillation degeneracies due to flavor oscillations before BBN the limit on L in the muon and tau neutrino sector strengthens. Then BBN constraint reads [23] $|\xi_\nu| < 0.1$. A more recent study for that case gives the constraint : $-0.04 < \xi_{\nu_e} < 0.07$ [24]. For such a small L the expansion rate remains practically standard because $\delta N_{eff} \sim 10^{-3}$.

However, it was realized later that the equilibration of the chemical potentials before BBN depends on the value of the yet unknown mixing θ_{13} . [25]. Besides, since relic L is capable to suppress or enhance oscillations, depending on its value and the values of oscillation parameters, L itself may play the role of an inhibitor or a catalyzer of the equilibration. Hence, different possibilities for the chemical potential in different neutrino flavors still may have place.

The analysis on the basis of BBN and D and ${}^4\text{He}$ abundance and CMB/LSS constraints on baryon-to-photon value, provided restrictive constraints on the neutrino degeneracy [11]. Namely the following constraints were derived for $N_{eff} = 3.3^{+0.7}_{-0.6}$ and different possibilities for the chemical potentials: in case $\xi_{\nu_e} \neq \xi_{\nu_\mu} = \xi_{\nu_\tau}$ $\xi_\nu < 2.3$ corresponding to $L < 5$; in case $\xi_{\nu_e} = \xi_{\nu_\mu} \neq \xi_{\nu_\tau}$ $\xi_{\nu_\tau} < 4$ $L < 7.6$, while in case $\xi_{\nu_e} = \xi_{\nu_\mu} = \xi_{\nu_\tau}$ $0.01 < \xi_\nu < 0.1$ and $L < 0.07$. In the last case practically the rate of expansion does not change, and the small dynamical effect of L corresponding to $\Delta N_{eff} \sim 0.03$ is undetectable by BBN and CMB [14].

CMB and LSS provide much looser bounds: L modifies the power spectra of radiation and matter [9],[15]. However, today's sensitivity of CMB and LSS data does not allow to probe different flavors.

² The possibility of L to suppress neutrino oscillations was discussed in the case of oscillations with larger mass differences first in ref. [21].

³The case of fast oscillations generating high enough L that exerts direct kinetic effect B on BBN was discussed in many publications (see for example ref. [22]).

They feel only the change in the total density, i.e. δN_{eff} . CMB data (including WMAP 5 years data results) combined with LSS data puts the bound: $\xi_\nu < 0.7$ and $L < 0.6$ at 2σ level.

The WMAP5 data combined with the data on BBN produced helium-4 provides more stringent bounds, namely: $-0.04 < \xi_\nu < 0.02$ in case of equilibration, while otherwise $-0.03 < \xi_{\nu_e} < 0.13$, $|\xi_{\nu_{\mu,\tau}}| < 1.67$ [10]. See however the recent work [26] based on the new data on Y_p and WMAP7, which allows considerable relaxation of the constraints, namely $-0.14 < \xi_{\nu_e} < 0.12$.

In conclusion, depending on the different combinations of observational data sets used and the assumed uncertainties, cosmology provides an upper bound for L in the range $|L_{\nu_{\mu,\tau}}| < 10^{-2} - 10$ and $|L| < 0.01 - 0.2$. These values are many orders of magnitude larger than the baryon asymmetry value.

In the next sections we analyze the effect of small L on BBN with late neutrino oscillations and present a possibility for much sensitive leptometer capable to constrain L values closer to the baryon one. Namely, we describe a model of BBN with late electron-sterile neutrino oscillations, which can 'measure' L as small as $L = 10^{-8}$.

3 Small Lepton Asymmetry and Late Neutrino Oscillations

Here we present the results on the interplay between small asymmetries $L \ll 0.01$ and late $\nu_e \leftrightarrow \nu_s$ oscillations in the early Universe and their effect on BBN. This study continues and broadens the analysis of refs. [17] and [19].

The effect of large L either previously existing or produced by oscillations, which effect directly the kinetic of BBN has been studied in numerous papers. The effect of small relic asymmetry was not so thoroughly studied. Its effect on primordial ^4He abundance was first analyzed for hundreds of $\delta m^2 - \theta$ combinations in refs. [17] and [2, 19].

We have analyzed electron-sterile neutrino oscillations

$$\begin{aligned}\nu_1 &= \cos(\theta)\nu_e + \sin(\theta)\nu_s \\ \nu_2 &= -\sin(\theta)\nu_e + \cos(\theta)\nu_s,\end{aligned}$$

where θ is the mixing angle, ν_1 and ν_2 are the Majorana particles with masses m_1 and m_2 . The sterile neutrino ν_s is not having the usual weak interactions, and is assumed to have decoupled much earlier than the flavor neutrinos, hence its density is much lower than the density of electron neutrino $n_{\nu_s} \ll n_{\nu_e}$. The case of neutrino oscillations effective after active neutrino decoupling $\delta m^2 \sin^4 2\theta \leq 10^{-7} \text{ eV}^2$ is studied in detail.

For that specific case of small L both the dynamical effect A , discussed in the previous section, and the direct kinetic effect B on nucleon kinetics are negligible. We will discuss the asymmetry effect C on oscillating neutrinos and through them on BBN.

In the case of late oscillating active-sterile neutrinos with relic or generated in oscillations L the energy distribution of neutrinos may be strongly distorted from the equilibrium Fermi-Dirac form [19]. Hence, a precise account for the energy spectrum distortion of the degenerate oscillating neutrinos is necessary to reveal the effect of small lepton asymmetry. Particularly the capability of small relic L to enhance oscillations has essentially spectral character [17] and requires a precise kinetic approach, provided in the numerical analysis, described below.

We have studied two different cases of L , namely initially present at the neutrino decoupling epoch, called further on relic L , and dynamically generated L by oscillations.

3.1 Evolution of Oscillating Neutrino in Presence of Lepton Asymmetry

We have used a self consistent numerical analysis of the kinetics of the oscillating neutrinos, the nucleons freeze-out and the asymmetry evolution for the analysis of lepton asymmetry role in BBN. Kinetic

equations for neutrino density matrix and neutron number densities in momentum space are used to describe the evolution of the system of oscillating neutrinos in the high temperature Universe, following the approach of ref. [2].

$$\begin{aligned}
\partial\rho(t)/\partial t &= H p_\nu (\partial\rho(t)/\partial p_\nu) + \\
&\quad + i[\mathcal{H}_o, \rho(t)] + i\sqrt{2}G_F (\mathcal{L} - Q/M_W^2) N_\gamma [\alpha, \rho(t)] + \mathcal{O}(G_F^2), \\
\partial\bar{\rho}(t)/\partial t &= H p_\nu (\partial\bar{\rho}(t)/\partial p_\nu) + \\
&\quad + i[\mathcal{H}_o, \bar{\rho}(t)] + i\sqrt{2}G_F (-\mathcal{L} - Q/M_W^2) N_\gamma [\alpha, \bar{\rho}(t)] + \mathcal{O}(G_F^2), \\
\partial n_n/\partial t &= H p_n (\partial n_n/\partial p_n) + \\
&\quad + \int d\Omega(e^-, p, \nu) |\mathcal{A}(e^- p \rightarrow \nu n)|^2 [n_{e^-} n_p (1 - \rho_{LL}) - n_n \rho_{LL} (1 - n_{e^-})] \\
&\quad - \int d\Omega(e^+, p, \tilde{\nu}) |\mathcal{A}(e^+ n \rightarrow p \tilde{\nu})|^2 [n_{e^+} n_n (1 - \bar{\rho}_{LL}) - n_p \bar{\rho}_{LL} (1 - n_{e^+})].
\end{aligned}$$

$\alpha_{ij} = U_{ie}^* U_{je}$, $\nu_i = U_{il} \nu_l$ ($l = e, s$). \mathcal{H}_o is the free neutrino Hamiltonian. Q arises as an W/Z propagator effect, $Q \sim E_\nu T$. $\mathcal{L} \sim 2L_{\nu_e} + L_{\nu_\mu} + L_{\nu_\tau}$, $L_{\mu,\tau} \sim (N_{\mu,\tau} - N_{\bar{\mu},\bar{\tau}})/N_\gamma$, $L_{\nu_e} \sim \int d^3p (\rho_{LL} - \bar{\rho}_{LL})/N_\gamma$.

The first two equations describe the evolution of neutrino and antineutrino ensembles. They provide a *simultaneous account* of the different competing processes: expansion (first term), neutrino oscillations (second term), neutrino forward scattering and weak interaction processes. The number densities of nucleons and electron neutrino were assumed the equilibrium ones. The sterile state was assumed empty at the time of decoupling of the electron neutrino.⁴

Due to the non-zero L term the equations are coupled integro-differential and the numerical task is much complicated than in the case of zero L . Besides, L term leads to different evolution of neutrino and antineutrino due to the different sign with which it enters their equations. (The case of $L \beta$ corresponds to negligible \mathcal{L} term in the potential when the evolution of the neutrino and antineutrino density matrices is identical.

We studied numerically the evolution of neutrino ensembles, evolution of L , and also the evolution of nucleons and L role during pre-BBN epoch for a broad range of oscillation parameters and $10^{-10} < L < 0.01$ for the case of a relic L . For the case of oscillations generated L its initial value was assumed $L \beta$. The numerical analysis was provided for the temperature range [0.3 MeV, 2 MeV] and the full set of oscillation parameters of the electron-sterile oscillations model, and with higher accuracy than in previous studies. We have calculated precisely neutron to nucleons freezing ratio $X_n^f = n_n^f/(n_n + n_p)^f = f(\delta m^2, \sin^2 2\theta, L)$ which is essentially influenced by oscillations and L . The primordially produced ${}^4\text{He}$ was estimated from it.

Active-sterile oscillations proceeding after neutrino decoupling produce ν_s at the expense of active neutrino and thus δN_{eff} does not change. However in that case late oscillations for a wide range of values of oscillations parameters and L , strongly distort neutrino energy spectrum. Therefore, a precise description of neutrino momenta distribution is necessary. In this analysis we have used between 1000 and 5000 bins to describe neutrino spectrum distribution in the non-resonant neutrino oscillations case, and up to 10 000 in the resonant case. Depending on the oscillation parameters and L values, the following interplay between L and oscillations can be observed: relatively large L suppress oscillations, smaller L lead to their resonant enhancement. On the other hand, resonant oscillations also are capable

⁴ the case of non-zero population of the sterile neutrino state was considered in detail for $L = 10^{-10}$ case in refs. [27, 28, 29]

to amplify L . In the following section we present the results of a detail numerical study of this interplay on BBN produced ${}^4\text{He}$.

4 Lepton Asymetry, Neutrino Oscillations and BBN. The Results

To study the lepton asymmetry effect on BBN we have provided a detail numerical analysis of the influence of L on Y_p , because primordially produced ${}^4\text{He}$ is highly sensitive to the nucleons kinetics during the pre-BBN epoch and besides, it is the most precisely measured element among light elements synthesized during BBN. A recent measurement of Y_p was provided on the basis of 93 spectra of 86 low redshift HII regions [4].

4.1 Oscillations Generated Lepton Asymmetry and BBN

In the analyzed oscillations case the evolution of L is dominated by neutrino oscillations and typically L has rapid oscillatory behavior: it oscillates and changes sign. We have determined numerically the region of parameter space for which noticeable generation of LA is possible. A good approximation is $|\delta m^2| \sin^4 2\theta \leq 10^{-9.5} \text{ eV}^2$. The maximal possible growth of L is by 4 -5 orders of magnitude. The instability region and the magnitude of L are close to the bounds existing in literature for other oscillation models [30].

Precise description of the distribution of the neutrino momenta was found extremely important for the correct determination of L evolution in the resonant oscillations case. In some cases increasing the resolution of momentum space leads to changes of the oscillatory character of L and diminishes L amplitude. ⁵ This observation is in accordance with the studies of other authors in other parameter regions corresponding to smaller θ and bigger δm^2 [31]. Further analysis is required to decide if the oscillatory behavior and strong asymmetry growth is induced by numerical error. This observation revives the puzzle: Is the asymmetry growth due to lack of numerical accuracy?!

L changes energy spectrum distribution and the number densities of electron neutrinos from standard BBN case. This influences the kinetics of nucleons during BBN and changes the production of light elements.

We have precisely followed the evolution of nucleons in the presence of electron-sterile neutrino oscillations in the pre-BBN period for different sets of oscillation parameters and different values of L . The production of ${}^4\text{He}$ was numerically calculated and compared to the BBN value without asymmetry growth account.

Fig. 1 illustrates the typical behavior of the frozen neutron number density relative to nucleons when increasing the mixing in case of asymmetry growth (red curves) and in case without asymmetry growth account for two different mass differences. The asymmetry growth takes place at smaller mixing angles when increasing δm^2 . Then *due to the asymmetry growth the production of X_n (correspondingly Y_p) decreases at small mixing*. The effect of the asymmetry growth on helium production is always towards decreasing of the caused by oscillations overproduction of ${}^4\text{He}$, leading to a relaxation of BBN constraints at small mixings.

In case of the small lepton asymmetry values, discussed here, BBN constraints on neutrino oscillations may notably change [19, 28, 29]. They become less stringent at small mixing angles (where the growth of asymmetry takes place).

Thus, the analysis has proven that BBN is sensitive to the oscillations generated asymmetry, which usually grow not more than 5 orders of magnitude and are small $|L| < 10^{-5}$.

⁵As a rule in these cases the evolution of the neutrino ensembles is strongly distorted from the expected behavior.

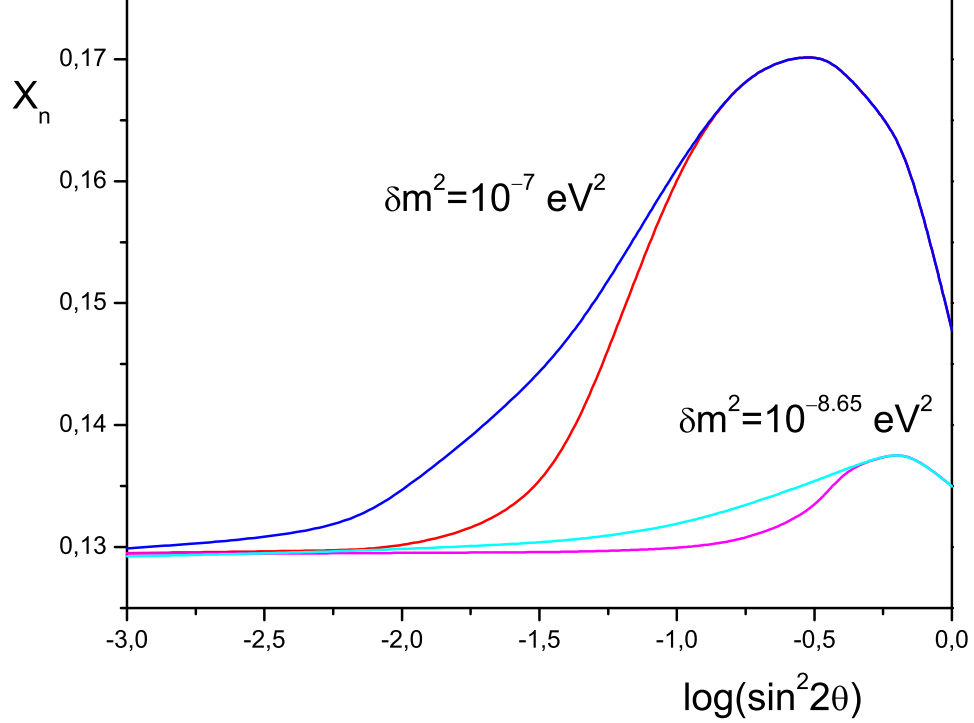


Figure 1: The dependence of the frozen neutron number density relative to nucleons on the mixing in case of the account of asymmetry growth (red curves) and in case without asymmetry growth account for two different mass differences $\delta m^2 = 10^{-8} \text{ eV}^2$ and $\delta m^2 = 10^{-7} \text{ eV}^2$.

4.2 Initial asymmetry, oscillations and BBN

Numerical analysis of $Y_p(\delta m^2, \theta, L)$ dependence has been provided for the entire range of mixing parameters of the model and relic $L \geq 10^{-10}$. Small L , $10^{-8} < L \ll 0.01$, that do not effect directly BBN kinetics, influence indirectly BBN via oscillations in agreement with previous analysis [17].

The calculated ${}^4\text{He}$ production dependence on oscillation parameters and on L shows that, in case of neutrino oscillations: i) BBN can feel extremely small L : down to 10^{-8} . ii) Large enough L change primordial production of ${}^4\text{He}$ by enhancing or suppressing oscillations. Depending on oscillation values $L \geq 10^{-7}$ may enhance oscillations, while $L > 0.1(\delta m^2/\text{eV}^2)^{2/3}$ may suppress oscillations, and asymmetries as big as $L > (\delta m^2/\text{eV}^2)^{2/3}$ inhibit oscillations. L enhancing oscillations leads to a higher production of Y_p . L suppressing oscillations decreases Y_p overproduction by oscillations. L bigger than 10^{-4} leads to a total suppression of oscillations, i.e. to the standard BBN yield of Y_p , without oscillations.

In Fig.2 the dependences of X_n^f on relic L for different mixings (to the left) and different mass differences are presented. For L smaller than $\sim 10^{-7}$ X_n^f keeps unchanged from the case without L . The higher the mixing - the higher is the overproduction of He-4 due to oscillations. Increasing further L for fixed oscillation parameters leads first to an increase of helium production, corresponding to the region of parameters space where L enhances oscillations, and then to a decrease of helium production, corresponding to big L suppressing oscillations, and hence to less Y_p overproduction caused by oscillations. At some critical L value defined by the concrete set of oscillation parameters $L_c(\delta m^2, \theta)$

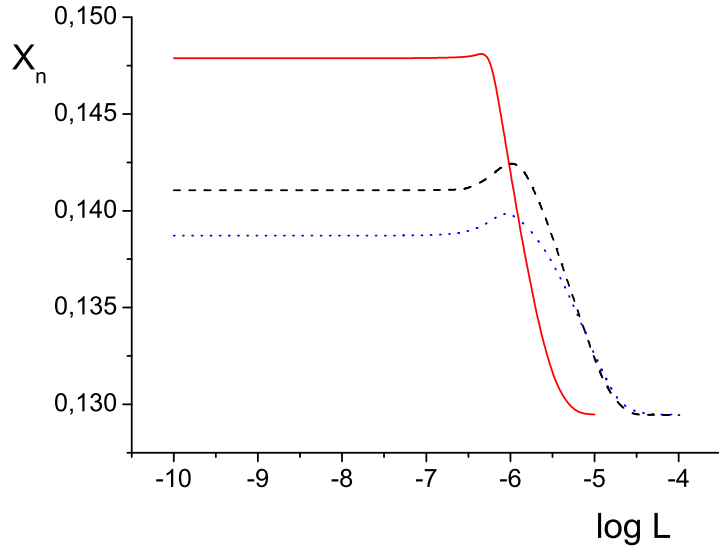


Figure 2: Frozen neutron number density relative to nucleons as a function of the relic initial lepton asymmetry for $\delta m^2 = 10^{-7} \text{ eV}^2$. The solid curve corresponds to maximal mixing, the dashed curve to $\sin^2 2\theta = 10^{-0.05}$ and the dotted curve to $\sin^2 2\theta = 10^{-0.1}$.

the produced helium reaches its standard BBN value - i.e. L has stopped the oscillations. As is illustrated in the figure, the width of the enhancement region and the height of the overproduction peak is sensitive to the mixing. Bigger values (up to about an order of magnitude) for L_c are necessary to inhibit oscillations when decreasing the mixing.

Fig.3 illustrates the dependence of X_n on the initial asymmetry value for a fixed mixing, namely $\sin^2 2\theta = 10^{-0.05}$ and different mass differences $\delta m^2 = 10^{-8} \text{ eV}^2$ and $\delta m^2 = 10^{-7} \text{ eV}^2$. The enhancement peak due to L is more clearly expressed for higher mass differences, and L_c is bigger for bigger mass differences. L bigger than $\sim 10^{-4}$ leads to a total suppression of oscillations effect on BBN for late oscillations studied here and hence, eliminates the BBN bounds on oscillation parameters. In that case instead the following approximate bound holds: $\delta m^2 / \text{eV}^2 < L^{3/2}$.

Depending on its value, relic L may also change BBN bounds: It relaxes them at large mixings and strengthens them at small mixings, as illustrated in ref. [17]

The next Fig.4 presents the dependence of X_n on the mass differences at a fixed non maximal mixing angle and for two different initial L . As illustrated, higher initial L leads to an increase of helium production at bigger mass differences, and reduces helium production at smaller mass differences. Correspondingly, increasing L at a fixed mixing leads to relaxation of the bounds at small mass differences and strengthens them at big mass differences.

At maximal mixing, however, bigger L leads to a suppression of the production of helium for all mass differences, and $L = 10^{-5}$ is enough to eliminate oscillations effect, i.e. to eliminate also the constraints on oscillation parameters in the discussed BBN model (see Fig.5).

Finally in Fig.6 we present the dependence of the helium production on the mixing angle at different initial L . Bigger L leads to decreasing the production of ^4He with increasing the mixing. I.e. for fixed mass differences, L relaxes the BBN constraints at large mixings. Analysis at bigger mass differences $\delta m^2 > 10^{-8} \text{ eV}^2$ has shown that at fixed δm^2 L strengthens the constraints at small mixing. The results are in agreement with the conclusions of ref.[17], where

the change of BBN bounds on neutrino oscillations in the presence of relic L was studied, namely:

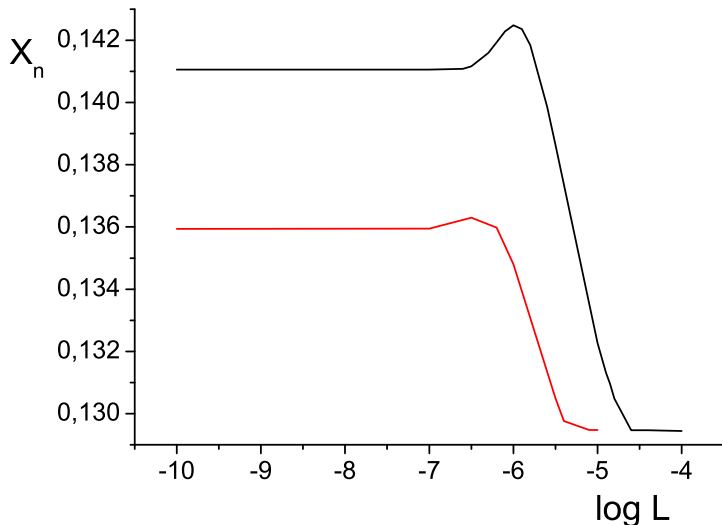


Figure 3: Frozen neutron number density relative to nucleons dependence on the initial asymmetry for $\sin^2 2\theta = 10^{-0.05}$ and two different mass differences $\delta m^2 = 10^{-8}$ eV² (lower curve) and $\delta m^2 = 10^{-7}$ eV² (upper curve).

L relaxes BBN bounds at large mixings and strengthens them at small mixings.

In conclusion, both small asymmetry generated by neutrino oscillations and small relic asymmetry influences the model of BBN with oscillations, because the produced primordially ${}^4\text{He}$ in this model feels extremely small L , namely $10^{-8} \geq L \ll 0.01$. Hence, BBN with oscillations presents a precise leptometer.

5 Summary

The lepton asymmetry of the Universe may be much bigger than the baryon asymmetry, and hidden in the neutrino sector. Since relic neutrino background is not yet detected, the lepton asymmetry in the neutrino sector may be measured/constrained just indirectly, namely by its influence on Universe expansion, Big Bang Nucleosynthesis, Cosmic Microwave Background, LSS, etc.

We discuss the case of small lepton asymmetry influence on the neutrino involved processes in pre-BBN epoch, and particularly on neutrino oscillations and BBN.

We have provided a detail numerical analysis of the interplay between small lepton asymmetry $L \ll 0.01$, either relic (initially present) or dynamical (generated by MSW active-sterile neutrino oscillations) and oscillating neutrino for the case of active-sterile neutrino oscillations occurring after electron neutrino decoupling. The evolution of asymmetry growth in case of small mass differences and relatively big mixing angles was studied in more detail. Higher resolution for the description of the neutrino momenta distribution is required for the investigation of the asymmetry behavior in this oscillation parameter region. The instability region in the oscillation parameter space, where considerable growth of L takes place, was determined numerically. In the case of relic lepton asymmetry we have determined the parameter range for which L is able to enhance, suppress or inhibit neutrino oscillations.

Cosmological influence of such small lepton asymmetries, which do not have direct effect on nucleons kinetics during BBN and are invisible by CMB, is discussed and shown to be considerable. Lepton

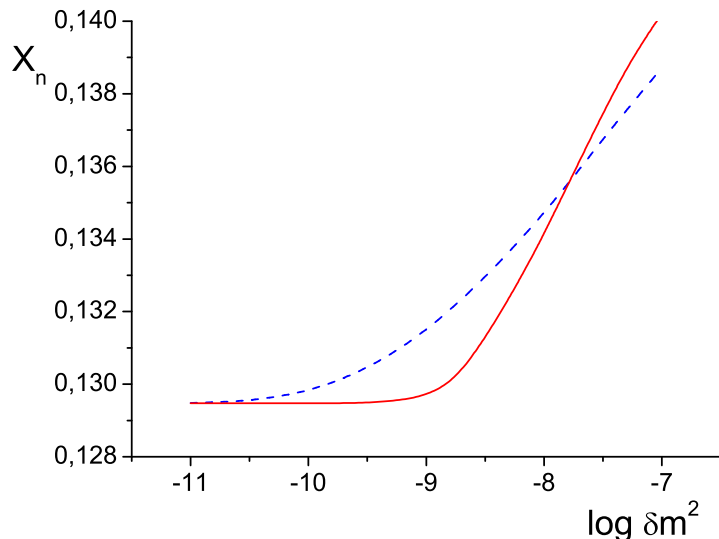


Figure 4: The dependence of the frozen neutron number density relative to nucleons on the mass differences at $\sin^2 2\theta = 10^{-0.1}$ and for two different initial lepton asymmetries $L = 10^{-10}$ (the dashed curve) and $L = 10^{-6}$ (solid curve).

asymmetries as small as 10^{-7} may be felt by BBN in case of neutrino oscillations. The effect of the dynamically generated and initially present L on BBN with oscillations was studied. Relic L present during BBN, depending on its value, may increase, decrease overproduction of Y_p or reduce it to the standard BBN value. Correspondingly, it can strengthen, relax or wave out BBN constraints on oscillations. It relaxes BBN bounds at large mixing and strengthens them at small mixings. Large enough L alleviates BBN constraints on oscillation parameters. In that case, instead, L constraint on oscillation parameters are derived.

Oscillations generated asymmetry at small mixing angles decreases the production of Y_p and relaxes BBN constraints at these angles.

The discussed model of BBN with late neutrino oscillations is sensitive to extremely small L .

Acknowledgements. I would like to thank M. Chizhov for the overall help during the preparation of this paper.

I acknowledge the travel support by the Bulgarian foundation "Theoretical and Computational Physics and Astrophysics" and the EPS grant supporting my stay at Centro Ettore Majorana during September 16-24, 2010 where this work was finalized.

References

- [1] R. Foot, M. Thomson, R. Volkas, *Phys. Rev. D* 53 (1996) R5349 .
- [2] D. Kirilova, M. Chizhov, *Neutrino96*, 478 (1996) D. Kirilova, M. Chizhov, *Phys. Lett. B* 393 (1997) 375 .
- [3] J. Hamann, S. Hannestad, G. Raffelt, I. Tamborra, Y. Wang *Phys. Rev. Lett.* 105 (2010) 181301
- [4] Y. Izotov T. Thuan, *Astrophys. J.* 710 (2010) L67
- [5] E. Komatsu et al. (WMAP), *Astrophys. J. Suppl.* 180 (2009) 330
- [6] A. Dolgov, *Phys. Rept.* 370 (2002) 333

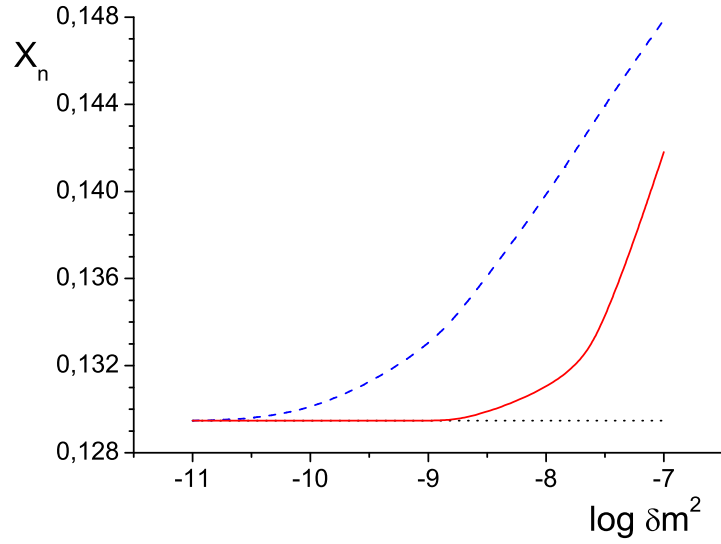


Figure 5: The dependence of the frozen neutron number density relative to nucleons on the mass differences at $\sin^2 2\theta = 1$ and for three different initial lepton asymmetries $L = 10^{-10}$ (the dashed curve) and $L = 10^{-6}$ (solid curve) and $L = 10^{-5}$ (the dotted curve).

- [7] Yi-Zen Chu, Marco Cirelli, *Phys. Rev. D* 74 (2006) 085015 A. Strumia, F. Vissani, hep-ph/0606054
- [8] S. Hannestad *Prog. Part. Nucl. Phys.* 65 (2010) 185 S. Hannestad *Ann. Rev. Nucl. Psrt. Sci.* 56 (2006) 137
- [9] J. Lesgourgues, S. Pastor *Phys. Rev. D* 60 (1999) 103521 ; *Phys. Rep.* 429 (2006) 307
- [10] M. Shiraishi, K. Ichikawa, K. Ichiki, N. Sugiyama, M. Yamaguchi, *JCAP* 0907 (2009) 005
- [11] Simha, G. Steigman, *JCAP* 0808 (2008) 011
- [12] P. di Bari astro-ph/0302433 v.3 2003 *Phys.Rev. D*67 (2003) 127301
- [13] R. Wagoner, W. Fowler, F. Hoyle, *Astrophys. J.* 148 (1967) 3 ; M. Smith, L.Kawano, R. Malaney, *Astrophys. J. Suppl.* 85 (1993) 219 ; H. Reeves, *Phys. Rev. D* 6 (1972) 3363 ; A. Yahil, G. Beaudet, *Astrophys. J.* 206 (1976) 26 ; G. Beaudet, P. Goret, *Astron. Astrophys.* 49 (1976) 415 ; K. Olive, D. Schramm, D. Thomas, T. Walker, *Phys. Rev. Lett.* B265 (1991) 239 ; H. Kang, G. Steigman, *Nucl. Phys. B* 372 (1992) 494 ; T. Kajino, M. Orito, *Nucl. Phys. A* 629 (1998) 538C
- [14] S. Pastor, T. Pinto, G. Raffelt, *Phys. Rev. Lett.* 102 (2009) 241302
- [15] L. Popa, A. Vasile *Rom. Rep. Phys.* 61 (2009) 531
- [16] D. Schwarz, M. Stuke, *JCAP* 0911 (2009) 025
- [17] D. Kirilova, M. Chizhov, *Nucl. Phys. B* 534 (1998) 447 .
- [18] X. Shi, *Phys. Rev. D* 54 (1996) 2753
- [19] D. Kirilova, M. Chizhov, *Nucl. Phys.B* 591 (2000) 457
- [20] D. Kirilova, M. Chizhov, in *Verbier 2000, Cosmology and particle physics*, 433 (2001), astro-ph/0101083
- [21] R. Foot, R. R. Volkas *Phys. Rev. Lett.* 75 (1995) 4350 ; *Phys. Rev. D* 55 (1997) 5147
- [22] R. Foot, R. R. Volkas, *Phys. Rev. D* 56 (1997) 6653 ; *Phys. Rev. D* 59 (1999) 029901
- [23] A. Dolgov, S. Hansen, S. Pastor, S. Petcov, G. Raffelt, D. Semikoz, *Nucl. Phys. B* 632 (2002) 363

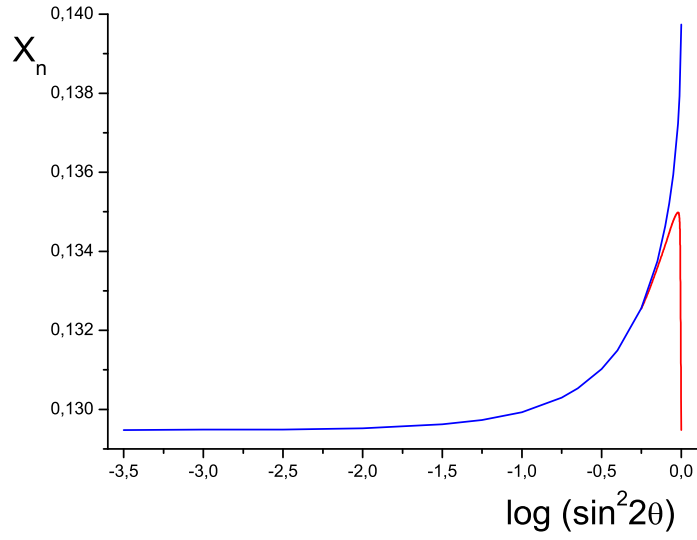


Figure 6: The dependence of the frozen neutron number density relative to nucleons on the mixing angle at $\delta m^2 = 10^{-8} \text{ eV}^2$ and for two different initial lepton asymmetries $L = 10^{-10}$ (the dashed curve) and $L = 10^{-6}$ (solid curve).

- [24] P. Serpico, G. Raffelt, *Phys. Rev. D* 71 (2005) 127301
- [25] S. Pastor, T. Pinto, G. Raffelt, *Phys. Rev. Lett.* 102 (2009) 241302 .
- [26] L. Krauss, C. Lunardini, C. Smith, arXiv:1009.4666 v2
- [27] D. Kirilova, *Int. J. Mod. Phys. D* 13 (2004) 831
- [28] D. Kirilova, *Int. J. Mod. Phys. D* 16 (2007) 1197
- [29] D. Kirilova, M. Panayotova, *JCAP* 12 (2006) 014
- [30] A. Dolgov, S. Hansen, S. Pastor, D. Semikoz, *Astropart. Phys.* 14 (2000) 79
- [31] P. Di Bari, R. Foot, *Phys. Rev. D* 61 (2000) 105012